Genotype-Phenotype Analysis of a Novel Recessive and a Recurrent Dominant SNRNP200 Variant Causing Retinitis Pigmentosa

Gerth-Kahlert, Christina ; Koller, Samuel ; Hanson, James V M ; Baehr, Luzy ; Tiwari, Amit ; Kivrak-Pfiffner, Fatma ; Bahr, Angela ; Berger, Wolfgang

Abstract: Purpose To compare phenotype variability in retinitis pigmentosa patients with recessive and dominant mutations in the SNRNP200 gene. Methods In a retrospective study, patients of two unrelated families were identified: family A, five patients aged 36 to 77 years; family B, one patient aged 9 years and his asymptomatic parents and sister. All patients received a comprehensive eye examination with a detailed retinal functional and morphologic assessment. Genetic testing was performed by whole exome sequencing (WES) in the index patient from each family. Genes described to be involved in eye diseases ($n > 450$) were screened for rare variants and segregation analysis was performed. Results A known heterozygous missense variant (c.3260C>T, p.(Ser1087Leu)) in the SNRNP200 gene was identified in the index patient of family A while a novel homozygous missense mutation (c.1634G>A, p.(Arg545His)) was found in the index patient of family B. Nyctalopia and photophobia were reported by 6/6 and 2/6 patients, respectively. The phenotype associated with the dominant mutation was characterized by variable disease onset (early childhood to the sixth decade of life), disease severity (visual acuity of 20/20-20/200 in the seventh to eighth decade), and advanced rod-cone dysfunction. Characteristics of recessive disease included distinct fundus changes of dot-like hypopigmentation together with retinal atrophy and severe rod-cone dysfunction. Conclusions The phenotype characteristics in autosomal dominant and recessive SNRNP200 mutations show distinct features, with earlier severe disease in the recessive case and a variable disease expression in the dominant inheritance pattern.

DOI: https://doi.org/10.1167/iovs.18-25643

DOI: https://doi.org/10.1167/iovs.18-25643

Genotype–Phenotype Analysis of a Novel Recessive and a Recurrent Dominant *SNRNP200* Variant Causing Retinitis Pigmentosa

Christina Gerth-Kahlert,[1] Samuel Koller,[2] James V. M. Hanson,[1] Luzy Baehr,[2] Amit Tiwari,[2] Fatma Kivrak-Pfiffner,[2] Angela Bahr,[2] and Wolfgang Berger[2–4]

[1]Department of Ophthalmology, University Hospital Zurich, Zurich, Switzerland
[2]Institute of Medical Molecular Genetics, University of Zurich, Schlieren, Switzerland
[3]Zurich Center for Integrative Human Physiology, University of Zurich, Zurich, Switzerland
[4]Neuroscience Center Zurich, University and ETH Zurich, Zurich, Switzerland

Correspondence: Christina Gerth-Kahlert, Department of Ophthalmology, University Hospital Zurich, Frauenklinikstrasse 24, 8091 Zurich, Switzerland; christina.gerth-kahlert@usz.ch.

Submitted: September 3, 2018
Accepted: May 9, 2019

Citation: Gerth-Kahlert C, Koller S, Hanson JVM, et al. Genotype–phenotype analysis of a novel recessive and a recurrent dominant *SNRNP200* variant causing retinitis pigmentosa. *Invest Ophthalmol Vis Sci*. 2019;60:2822–2835. https://doi.org/10.1167/iovs.18-25643

Purpose. To compare phenotype variability in retinitis pigmentosa patients with recessive and dominant mutations in the *SNRNP200* gene.

Methods. In a retrospective study, patients of two unrelated families were identified: family A, five patients aged 36 to 77 years; family B, one patient aged 9 years and his asymptomatic parents and sister. All patients received a comprehensive eye examination with a detailed retinal functional and morphologic assessment. Genetic testing was performed by whole exome sequencing (WES) in the index patient from each family. Genes described to be involved in eye diseases ($n > 450$) were screened for rare variants and segregation analysis was performed.

Results. A known heterozygous missense variant (c.3260C>T, p.(Ser1087Leu)) in the *SNRNP200* gene was identified in the index patient of family A while a novel homozygous missense mutation (c.1634G>A, p.(Arg545His)) was found in the index patient of family B. Nyctalopia and photophobia were reported by 6/6 and 2/6 patients, respectively. The phenotype associated with the dominant mutation was characterized by variable disease onset (early childhood to the sixth decade of life), disease severity (visual acuity of 20/20–20/200 in the seventh to eighth decade), and advanced rod-cone dysfunction. Characteristics of recessive disease included distinct fundus changes of dot-like hypopigmentation together with retinal atrophy and severe rod-cone dysfunction.

Conclusions. The phenotype characteristics in autosomal dominant and recessive *SNRNP200* mutations show distinct features, with earlier severe disease in the recessive case and a variable disease expression in the dominant inheritance pattern.

Keywords: SNRNP200, retinitis pigmentosa, autosomal dominant, autosomal recessive, genotype phenotype correlation

The gene small nuclear ribonucleoprotein U5 subunit 200 (*SNRNP200*) codes for a splicing factor, designated HELIC2, and is essential for unwinding of U4/U6 RNA duplices—an important step in the catalytic activation of the spliceosome.[1–3] The *SNRNP* mutation c.3260C>T, p.(Ser1087Leu) was initially described in two Chinese families with nonsyndromic autosomal dominant retinitis pigmentosa (RP).[4,5] Benaglio et al.[6] estimated a high prevalence of *SNRNP200* mutations among Caucasian autosomal dominant RP patients of at least 4.2%. A study among the French Canadian founder population revealed mutations in *SNRNP200* in 17% of the cases where a disease-associated mutation was detected (60 patients tested in total; 4 out of 17 mutations occurred in *SNRNP200*).[7] *SNRNP200* mutations were also identified in 1/163 (mutation frequency 0.6%) patients with cone-rod dystrophy (CORD).[8] Autosomal recessive inheritance has been suggested by several authors,[9–11] since homozygous[9,11] as well as possibly compound heterozygous mutations[10] in the *SNRNP200* gene have been identified. The reported range of phenotypes varies from Leber congenital amaurosis (LCA) caused by a homozygous mutation[9] to juvenile RP. A recent report by Zhou et al.[12] suggested an association between early-onset high myopia (eoHM) and heterozygous *SNRNP200* missense mutations, although no retinal functional testing in the reported patients was documented. Most of the mutations in the *SNRNP200* gene are missense mutations, with two exceptions: c.2036+1G>T affects the splice donor site of exon 15 and c.2941-2A>G the splice acceptor site of exon 22, as illustrated in Figure 1. Here, we elucidate and compare the retinal phenotype in patients with a previously described dominant *SNRNP200* mutation to an affected individual with a novel recessive *SNRNP200* variant.

Methods

This is a retrospective description and analysis of the genotype and phenotype of patients with mutations in the *SNRNP200* gene. This work was approved by the Cantonal Ethics Committee of Zurich and adhered to the tenets of the Declaration of Helsinki.

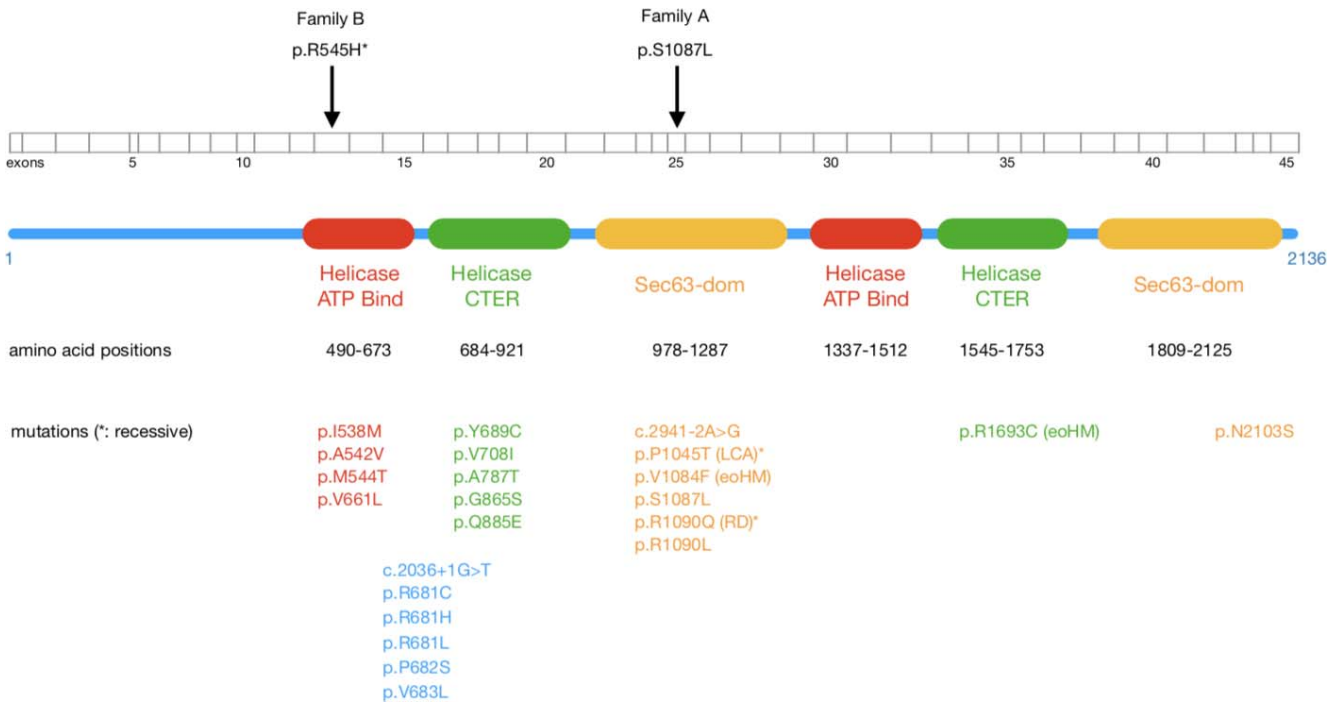

Figure 1. Schematic drawing of the SNRNP200 protein consisting of 2136 amino acid residues and their functional domains according to Zhang et al.[43] Disease-causing mutations are indicated at the protein level. Most of them are missense mutations, with two exceptions: c.2036+1G>T affects the splice donor site of exon 15 and c.2941-2A>G the splice acceptor site of exon 22. The majority of mutations are dominant and lead to retinitis pigmentosa except when indicated otherwise. Recessive mutations are indicated by an *asterisk*. RD, retinal dystrophy.

Ocular Phenotype

All patients were seen and examined in the course of the clinical practice of the first author (C.G-K.) between November 2016 and April 2018.

All patients and available family members received a full ophthalmologic examination including measurement of visual acuity, dilated fundoscopy, optical coherence tomography (OCT; Spectralis; Heidelberg Engineering GmbH, Heidelberg, Germany), kinetic perimetry (Octopus 900 or manual Goldmann perimeter; Haag-Streit AG, Köniz, Switzerland), full-field electroretinography (ff-ERG; Espion; Diagnosys LLC, Lowell, MA, USA), autofluorescence (AF) examination using the Optomap (Optos plc, Dunfermline, UK) and/or Heidelberg Spectralis, and fundus photography. In patients and affected family members with sufficient visual acuity and adequate fixation it was also possible to perform multifocal electroretinography (mf-ERG) with the Espion system also used for ff-ERG recording.

When possible, OCT was performed in high-resolution mode using a volume scan (31 horizontally aligned sections separated by 245 μm covering a retinal area of 30° horizontally × 25° vertically; 15 Automatic Real-time Tracking [ART] scans averaged) centered on the fovea. The precise settings used were amended when circumstances dictated (e.g., when poor vision or inability to maintain fixation in a patient or affected family member rendered the standard scans unfeasible); using this approach, it was possible to obtain some form of OCT scan, even if just a single section, in all patients and examined family members. All scans were inspected for segmentation errors by a single author (J.V.M.H.), and the definitions of the inner limiting membrane and Bruch's membrane were, when necessary, corrected. Due to afoveal fixation it was not possible to use the 1-, 3-, 6-mm Early Treatment Diabetic Retinopathy Study (ETDRS) grid when calculating total macular volume (TMV) in some patients with severe visual loss; therefore the 1-, 2.22-, 3.45-mm grid was employed for all patients instead, in order to facilitate comparison of TMV values across all patients who were able to yield a volume scan.

As with OCT, the precise nature of the kinetic perimetry examinations was dependent on the residual visual quality and consequent ability to perform the examination of the patients and affected family members. When possible, V4e, I4e, and I2e isopters were kinetically measured and verified with presentation of scattered static stimuli; as a minimum, V4e isopters were measured and statically verified.

Ff-ERG and mf-ERG were recorded according to published recommendations of the Society for Clinical Electrophysiology of Vision.[13] Medical mydriasis was accomplished using topical 0.5% tropicamide and 5% phenylephrine. Gold-plated skin electrodes at the ipsilateral outer canthi (reference) and center of the forehead (ground) were used, together with single-use Dawson-Trick-Litzkow recording electrodes (Diagnosys LLC). Before applying skin electrodes, the patients' skin was cleaned and scrubbed using ethanol-based hand disinfectant and an abrasive paste in order to minimize electrical impedance during recording. Topical 0.4% oxybuprocaine was instilled prior to positioning the DTL electrodes in order to minimize patient discomfort.

Recording of the ERG was preceded by a period of dark adaptation lasting 20 minutes. Following this, patients were presented with 0.01-cd/m^2 flashes ("rod") followed by 3.0-cd/m^2 flashes ("rod-cone") in order to measure the responses of the rod system and combined rod-cone systems, respectively. Patients were then adapted to a rod-bleaching 30-cd/m^2 light for 10 minutes before being presented with 3.0-cd/m^2 light, both flickering (30-Hz frequency; "cone flicker") and as single flashes (at a frequency of 1 Hz; "cone"). All stimuli were delivered via a diffusing full-field stimulator and were composed of white light. Multiple responses were recorded, which were assessed and accepted or rejected online in order

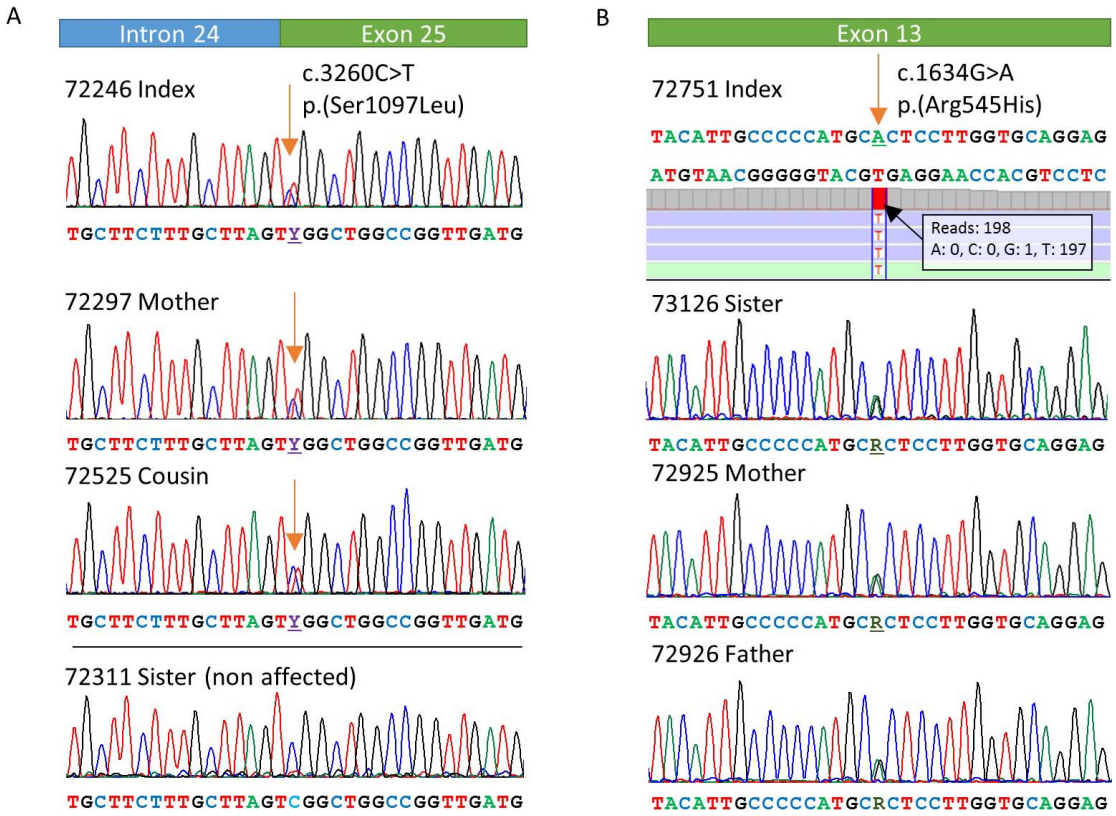

Figure 2. Sequencing analysis of *SNRNP200* (NM_014014.4) variants. (**A**) Sanger sequencing results of family A index patient, selected affected family members, and a representative nonaffected family member are shown. (**B**) WES analysis of family B index and Sanger sequencing results of the parents and sister of the index patient.

to verify reproducibility and ensure that the averaged potentials were uncontaminated by visible artifacts.

Recording of the mf-ERG was performed in normal room illumination using an achromatic 61-hexagon stimulus array covering approximately 50° of the central visual field. Individual hexagons had a luminance of either 400 or 0.0 cd/m^2, which was determined for each hexagon according to a 14-bit M-sequence at 75 Hz. Recordings were bandpass filtered (10–100 Hz) in order to remove extraneous electrical noise.[13] Each recording session lasted 30 seconds, with a minimum of eight sessions required to complete the mf-ERG recording.

Molecular Genetic Testing

DNA for whole exome sequencing (WES) was extracted from peripheral blood. Library preparation for next-generation sequencing (NGS) was performed according to the manufacturer's protocol using either Illumina (San Diego, CA, USA) Nextera Rapid Capture Exome (index patient of family A) or Illumina TruSeq Exome kit (index patient of family B). Paired-end NGS sequencing was performed on an Illumina NextSeq500 platform (cycles: 2×150 for index patient of family A, 2×75 for index patient of family B). Alignment and variant calling were performed on an Illumina BaseSpace on-site server. VCF files were annotated by using Alamut Batch (version 1.9; Interactive Biosoftware, Rouen, France) with an in-house gene list ($n = 483$) of known or potential candidate genes involved in eye diseases, in particular retinal disorders. Variants were filtered for either presence in the Human Gene Mutation Database (HGMD) or frequency (<1%) in the non-Finnish European population (gnomAD database, Lek et al.[14]). Missense variants were considered when they were predicted to be disease causing by at least three of the following five algorithms: Align GVGD, SIFT, MAPP, MutationTaster2, or PolyPhen2.

Copy number variation (CNV) analysis was performed by analysis of exome NGS data using cn.MOPS[15] and EXCAVATOR2[16] software.

Sanger sequencing was performed for segregation analysis as previously described by Haghighi et al.[17]

Results

Two unrelated families were identified with heterozygous (family A) or homozygous (family B) amino acid substitutions in the *SNRNP200* (NM_014014.4) gene (Fig. 2). The families were of Caucasian ethnicity, originating from Switzerland (family A) and Kosovo (family B), and both without known consanguinity (Fig. 3).

Family A: Autosomal-Dominant RP Caused by a Heterozygous Missense Mutation (c.3260C>T p.(Ser1087Leu)) in *SNRNP200*

Detailed data from five affected family members were available (Figs. 4–6; Tables 1, 2). The index patient III:1 was first examined at our institution because of intermittent exotropia, which resolved after subsequent strabismus surgery. Age at first symptoms varied between early childhood and around 55 years. All patients complained of nyctalopia as their first symptom, with photophobia developing in three of the five examined patients during their disease course. The index patient of this family (III:1) was first diagnosed at the age of 5

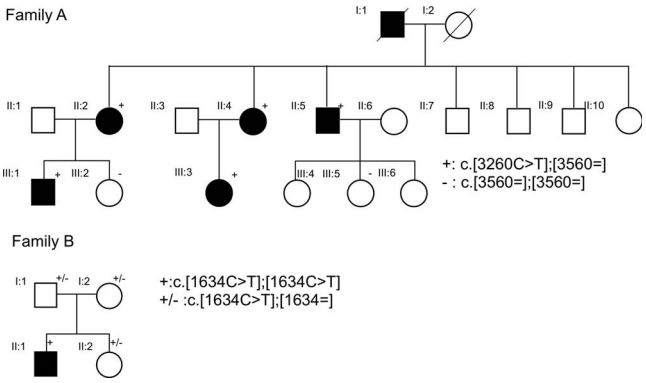

Figure 3. Pedigrees of the two unrelated families are shown. Consanguinity is not known in either family, originating in Switzerland (family A) and in Kosovo (family B).

years. He received parabulbar injections of benzyl-imidazoline at an outside institution between ages 5 and 12 years (according to the patient, in order to control the retinal disease), but no further information or documentation was available to us. All patients in this family reported a slow but relentless progression of their vision loss while nevertheless being able to study and maintain employment in demanding professions. The index patient and affected relatives were all moderately to highly myopic from early childhood onward (Table 1).

Best-corrected visual acuity ranged from 20/20 (patient II:2 at age 67) to 20/100 to 20/200 (patients II:4 and II:5 at ages 66 and 77, respectively) (Table 1). Patient II:5 experienced complete loss of vision (no light perception; NLP) in the right eye due to an intracerebral meningioma (no further details available). Analysis of the visual fields demonstrated an advanced midperipheral and nasal field loss in the fourth decade (III:1 and III:3) and a small residual central island only

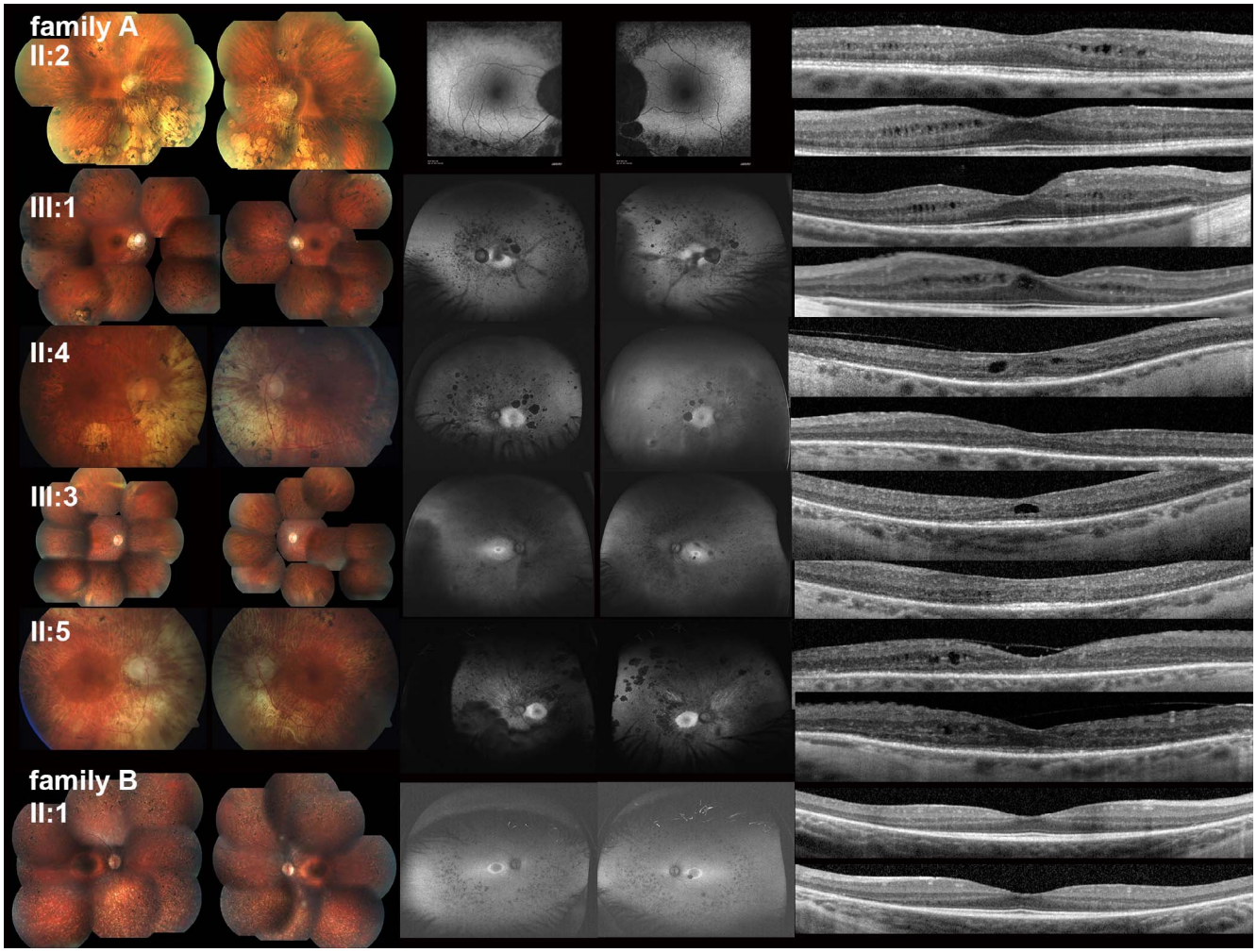

Figure 4. Retinal morphology (fundus photography, corresponding autofluorescence [AF] images, and horizontal spectral-domain OCT scans through the fovea, arranged from *left to right*, respectively) of both eyes is shown for all affected patients from family A and the one patient of family B. OCT scans are displayed with the right eye uppermost for each patient. Composite fundus photography of patient II:2 shows mildly atrophic maculae, midperipheral bone spicule pigmentation, central hyperAF, and cystoid macular edema (CME) confined to the inner nuclear layer (INL). Patient III:1 shows less generalized, but already marked, circumscribed islands of chorioretinal atrophy, ring-shaped hyperAF, and CME. Patient II:4 displays generalized atrophy that is more severe nasally to the optic nerve head, ring-shaped hyperAF, cystic macular lesions in the right eye only, and reduced macular thickness in both eyes. Composite fundus photography in patient III:3 shows relatively little retinal atrophy in the presence of bone spicule pigmentary changes, moderate hyperAF, and a large cystic lesion in the foveal region in the right eye only. Patient II:5 shows a pattern of atrophy predominantly of the nasal retina and AF findings similar to patient II:4, extended macular atrophy, and CME with epiretinal membranes in both eyes. Composite fundus photography of patient II:1 (family B) reveals dotted hypopigmentation intermingled with bone spiculae, ring-shaped hyperAF at the maculae, and a maintained macular laminar structure without CME or visible cystic lesions.

Investigative Ophthalmology & Visual Science

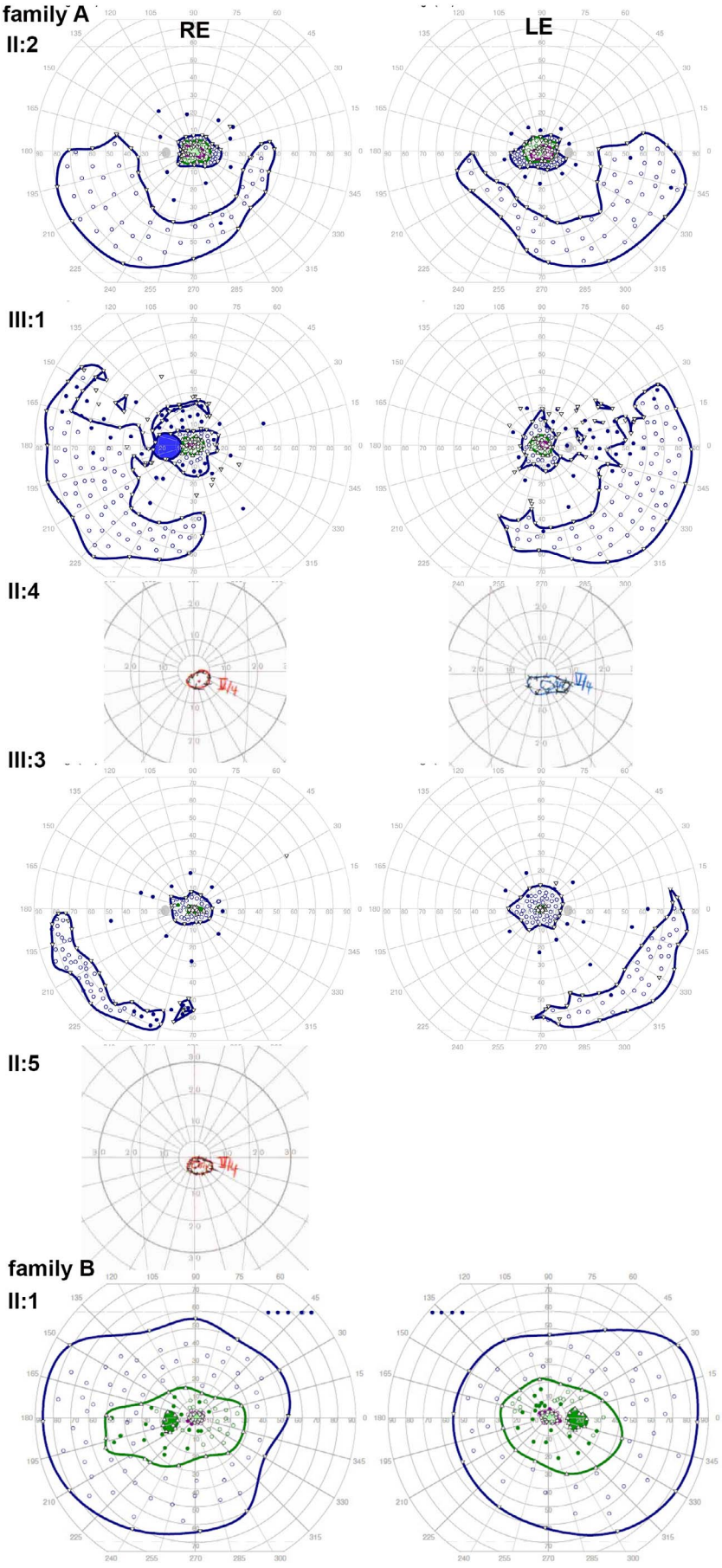

Investigative Ophthalmology & Visual Science

Figure 5. Kinetic visual fields are shown for all affected patients of family A and the one patient of family B. In family A, patients II:2, III:1, and III:3 show intact peripheral islands of varying extent, predominantly inferiorly and/or temporally. In contrast, patients II:4 and II:5 show residual central islands only. Note that patient II:5 has no light perception in the right eye following an intracerebral meningioma. Patient II:1 from family B shows an almost normal visual field with the largest stimulus tested (V4e), otherwise constricted (I4e).

at older ages (II:4 and II:5). In contrast, perimetry in patient II:2 at age 67 years revealed a field loss with a residual central and inferior-temporal island similar to that recorded in her son at age 36 years (Fig. 5).

Ff-ERG results were consistent with rod-cone dysfunction, with recognizable but severely reduced and slightly delayed cone-mediated responses only in the index patient (III:1) aged 36 years. Here, the b-wave amplitude of the 3.0-cd/m^2 light-adapted (cone)[18] response measured only 7.5 and 11.7 μV (5th–95th percentile in our clinic: 101.5–263.5 μV) with a significantly delayed response peak time of 34.5 and 41 ms in the right and left eyes, respectively. Ff-ERG responses in his mother (patient II:2) at age 67 years were not delayed and were less severely affected, with recordable but severely reduced 3.0-cd/m^2 dark- and light-adapted responses, the latter being comparable in amplitude to those recorded contemporaneously in her son, despite an age difference of 31 years. Mf-ERG recordings revealed a normal (both eyes in II:2) to reduced (right eye in III:3) or delayed (left eye in III:1) central response, corresponding to a better-preserved visual acuity in the eyes with normal central mf-ERG responses (right eye in III:1; left eye in III:3, both eyes in II:2) (Fig. 6).

Typical fundus changes suggestive of retinal dystrophy were observed in all patients, although to a slightly lesser extent in the two patients in their fourth decade compared to the two older patients (aged 66 and 77 years) (Fig. 4). Bone spicule pigmentation was more obvious in the midperiphery and associated with mild maculopathy and optic disc pallor in patients III:1 and III:3, whereas patient III:1 showed typical tilted discs and peripapillary atrophy related to his high myopia. Advanced chorioretinal atrophy (nasally more than temporally), severe maculopathy, and atrophic optic discs were visible in patients II:4 and II:5, corresponding to their longer disease course at the time of examination. However, fundus changes in patient II:2 were less severe despite the patient's age of 67 years. Retinal AF shows increased autofluorescence within the central macula and reduced autofluorescence corresponding to the atrophic fundus changes in all patients. Analysis of the macular layers and their thicknesses revealed a maintained laminar structure with atrophic outer retinal layers and reduced central retinal thickness (CRT) and TMV (Table 2). The macular ellipsoid zone was preserved in three patients of different ages (III:1, III:3, II:2; 36, 37, and 67 years, respectively). Cystoid macular edema was apparent to a varying extent in all five patients within the extrafoveal inner nuclear layer and, in patients III:1 (left eye) and III:3 (right eye), also in in the parafoveal inner nuclear layer. None of the OCT scans demonstrated changes suggestive of outer retinal tubulations (Fig. 4).

Exome sequencing data analysis revealed a rare missense mutation (c.3260C>T, p.(Ser1087Leu)) in *SNRNP200*, which has been previously described[19] (Fig. 2) and confirmed as disease-associated through functional analysis.[3] This variant has a frequency of 1 in 246,000 alleles worldwide and 1 in 112,000 non-Finnish Europeans (gnomAD, August 2018). Segregation analysis of this sequence variant by Sanger sequencing was performed in the mother, unaffected sister, and affected aunt of the index patient (Tables 3, 4). The identified sequence variation in SNRNP200 was present in the mother and affected aunt, but absent in the unaffected sister. Additional sequence variations were detected in *UNC119* and *MYO7A* (Table 3). However, only the missense variation in *SNRNP200* segregated with RP in this family. The two compound heterozygous missense variations in *MYO7A* were detected only in the index patient (III:1) and may represent modifier alleles for the disease in this patient, who had normal responses on audiometry and no signs of vestibular dysfunction.

Family B: Autosomal Recessive RP Caused by a Homozygous Missense Mutation (c.1634G>A, p.(Arg545His)) in *SNRNP200*

The 10-year-old index patient of family B reported nyctalopia, beginning around 1 year before initial examination, as his only symptom. An avid football (soccer) player, he had not noticed changes in his vision or his ability to participate in games. On examination, his best-corrected visual acuity was subnormal at 20/40 in both eyes. Perimetry showed constricted kinetic isopters and a paracentral scotoma verified with static test points (Fig. 5). Ff-ERG confirmed a severe rod-cone dysfunction, with nonrecordable responses under scotopic conditions, minimal responses under photopic conditions, and a light-adapted 3.0-cd/m^2 (cone) b-wave response amplitude of 22.3 and 17.8 μm in the right and left eyes, respectively. Localized response analysis of the mfERG revealed normal cone-mediated responses within the central 5° in radius, but delayed and reduced responses outside this retinal area (Fig. 6). Retinal examination showed marked midperipheral to peripheral changes, with spotted or dot-like hypopigmentation, bone-spicule pigmentation, and retinal atrophy. OCT showed reduced retinal thickness, but no cystoid macular changes were observed. The thinning of the outer retinal layers, in particular of the ellipsoid zone, corresponded with a perimacular ring of increased autofluorescence (Fig. 4).

His asymptomatic parents (both aged 40) both demonstrated normal visual acuity, normal retinal morphology, and normal ff-ERG findings (perimetric testing was omitted in the parents due to these normal examination results).

Filtering of whole exome sequence data of 483 genes related to ocular, and in particular retinal, diseases revealed only one variant that also met the genetic criteria: c.1634G>A (p.(Arg545His)) in the *SNRNP200* gene (Tables 3, 4). This variant was observed in the homozygous state in the index patient and the heterozygous state in both parents and the asymptomatic sister (Fig. 2). No frequency data were found in public databases for this variant (Exome Sequencing Project Variants, ClinVar, COSMIC, dbSNP, gnomAD, 1000 Genomes). Prediction algorithms revealed the following values: Align GVGD[20] class C0 (GV 241.65, GD 1.62), SIFT deleterious[21] (score: 0.02), MutationTaster[22] disease causing (*P* value: 1), PolyPhen-2 probably damaging[23] (score: 0.999, sensitivity: 0.14, specificity 0.99), and MAPP bad[24] (*P* value 0.007, *P* value-median 0.003). In addition, EX-SKIP[25] predicts a higher probability of exon skipping for the variant compared to the reference sequence. These results make the nucleotide substitution c.1634G>A the most likely disease-causing variant in the index patient of family B. Other most likely non–disease-causing variants, which met filtering but not genetic criteria, are listed in Table 3. CNV data analysis did not reveal any suspicious alternations in the patient.

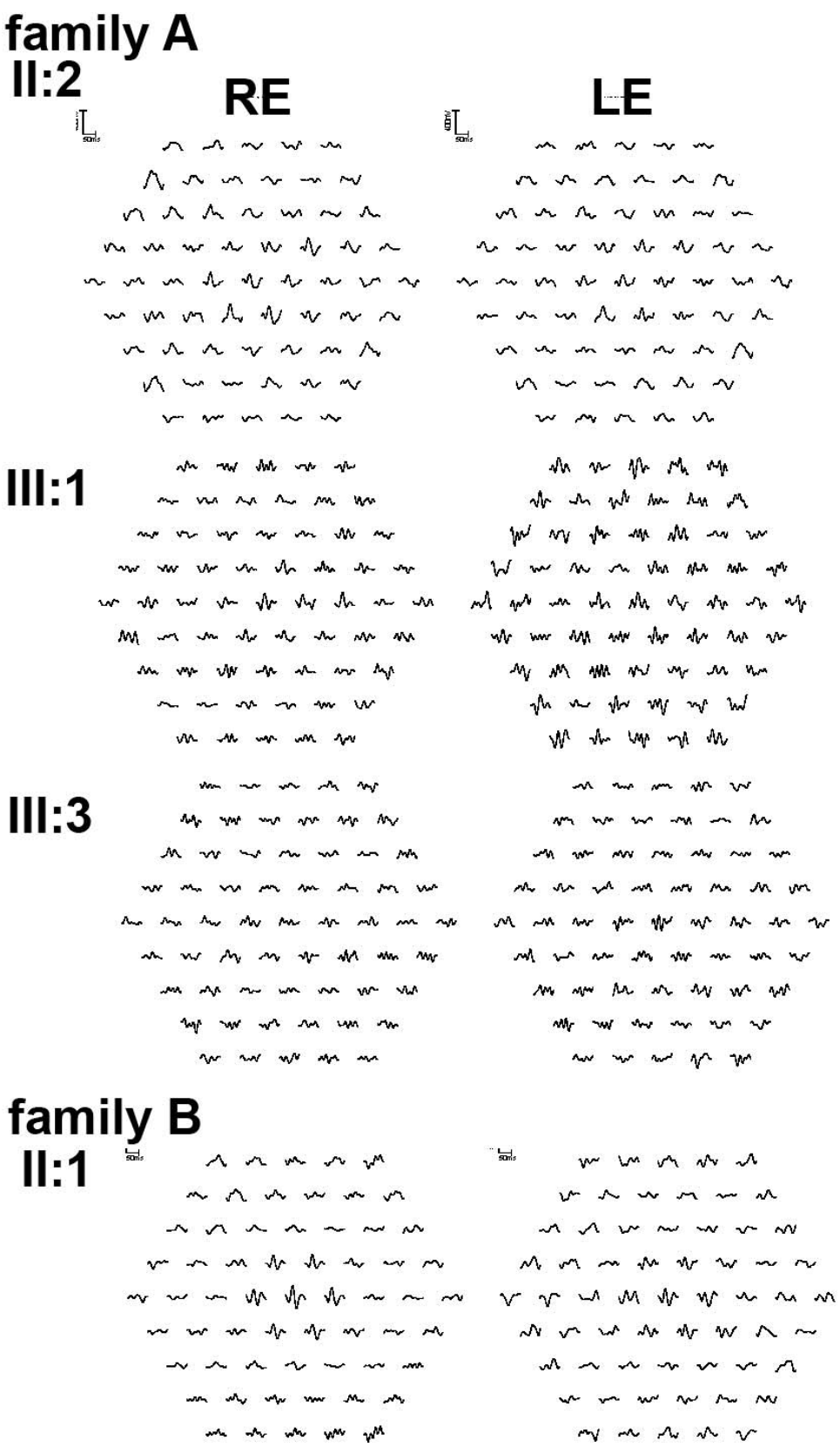

Figure 6. Multifocal ERG responses are shown for patients II:2, III:1, and III:3 of family A and patient II:1 of family B. All tested patients in family A show reduced to nonrecordable responses outside the central stimulus area, with normal (II:1 both eyes; III:1 right eye; III:3 left eye) to slightly abnormal (III:1 left eye delayed response; III:3 right eye reduced response) central responses. Patient II:1 of family B had normal responses in approximately the central 5°, with delayed and reduced responses outside this zone.

Investigative Ophthalmology & Visual Science

Table 1. Summary of Ocular Phenotype in Patients Studied

Patient ID	Family ID	Sex	Age at First Symptoms	Age at Visit	Photophobia	Nyctalopia	VA		Refraction, MSE		VF	ffERG	mfERG
							RE	LE	RE	LE			
II:2	1	F	Around age 55	67	−	+	20/20	20/20	+1.0	+0.5	20° (V4e), inferior and temporal "island".	Scotopic NR, photopic severely reduced responses.	Central response: normal, otherwise reduced but not delayed.
III:1	1	M	Early childhood	36	−	+	20/25	20/40	−10	−9	10° to 20°, temporal large field (V4e).	Scotopic NR, photopic severely reduced responses.	Central response: RE normal, LE delayed, otherwise reduced or within noise.
II:4	1	F	Around age 20	66	+	+	20/50	20/200	−10	−10	5° (V4e).	Not performed.	Not performed.
III:3	1	F	Around age 10	37	+	+	20/50	20/30	−2.25	−2.75	10° to 20°, temporal large areas (V4e).	Scotopic and photopic NR.	Central response: RE reduced, LE normal, otherwise nonrecordable.
II:5	1	M	7 y	77	−	+	NLP	20/100	−3.5	−1.75	5° (V4e).	Not performed.	Not performed.
II:1	2	M	9 y	10	−	+	20/40	20/40	+0.75	+0.75	Normal (V4e), concentric constriction (kinetic I4e) and paracentral scotomas (static I4e).	Scotopic NR, photopic severely reduced and delayed responses.	Central 5° responses normal, 10° to 25° delayed and reduced.

F, female; LE, left eye; M, male; MSE, mean spherical equivalent; NR, nonrecordable; RE, right eye; VA, visual acuity; VF, kinetic visual fields (horizontal for listed isopters).

Table 2. Retinal Morphology and SD-OCT Characteristics

Patient ID	Family ID	Age at Visit	Maculopathy	Fundus Periphery	AF	SD-OCT: CME	SD-OCT CRT, µm		SD-OCT TMV,* mm^3	
							RE	LE	RE	LE
II:2	1	67	Mild atrophy	Midperipheral bone spiculae and retinal atrophy, retinal vessel attenuation, optic disc with mild pallor.	Macula with hyperAF with central hypoAF, midperipheral speckled hypoAF.	+	273	261	2.93†	2.94†
III:1	1	36	Mild atrophy	Midperipheral bone spiculae and retinal atrophy, retinal vessel attenuation, tilted optic disc with mild pallor.	Central macula with large ring-shaped area of hyperAF with central hypoAF, midperipheral speckled hypoAF.	+	253	298	3.15	3.18
II:4	1	66	Severe atrophy	Bone spiculae and generalized retinal atrophy, retinal vessel attenuation, atrophic optic disc.	Central macula with large ring-shaped hyperAF with centrally slightly reduced hyperAF, midperipheral speckled hypoAF.	+	241	155	2.18†	2.15†
III:3	1	37	Mild atrophy	Midperipheral bone spiculae and retinal atrophy, retinal vessel attenuation, mild optic disc pallor.	Central macula area with moderate hyperAF filled with ring of hyperAF, midperipheral mild speckled hypoAF.	+	192	215	2.31†	2.31†
II:5	1	77	Severe atrophy	Midperipheral bone spiculae, severe retinal atrophy, retinal vessel attenuation, atrophic optic disc.	Central macula with ring-shaped hyperAF with centrally slightly reduced hyperAF, midperipheral speckled hypoAF.	+	NA	206	NA	2.5†
II:1	2	10	Mild atrophy	Midperipheral to peripheral bone spiculae and dotted hypopigmentation, retinal vessel attenuation.	Paracentral ring of hyperAF, midperipheral speckled hypoAF.	−	210	210	2.58†	2.52†

For comparison, the normal range of TMV using this ETDRS grid at our center (as defined by the 5th–95th percentiles calculated using 57 eyes of 57 healthy individuals) is 2.97 to 3.47 mm^3. NA, not available; SD-OCT, spectral-domain optical coherence tomography; +, present; −, absent.

* Derived from the 1-, 2.22-, 3.45-mm ETDRS grid.

† TMV values outside the normal range.

Table 3. Summary of Mutation Information of the Index Patient in Family A and B

Gene	Reference Sequence	Exon/Intron	RsID	GnomAD Freq.	DNA Level	Protein Level	Zyg.
Index patient family A							
SNRNP200	NM_014014.4	Exon 25	rs267607077	0%	c.3260C>T	p.(Ser1087Leu)	Het
UNC119	NM_005148.3	Exon 4a	rs146916036	0.1%	c.502C>T	p.(Arg168Cys)	Het
MYO7A	NM_000260.3	Exon 35	rs370232066	0.02%	c.4739A>G	p.(Tyr1580Cys)	Het
MYO7A	NM_000260.3	Exon 39	rs762836180	0.03%	c.5380G>A	p.(Glu1794Lys)	Het
Index patient family B							
ABCA4	NM_000350.2	Exon 6	rs757844726	0.013%	c.694C>T	p.(Leu232Phe)	Het
ADGRV1	NM_032119.3	Exon 28	rs41308846	0.80%	c.6133G>A	p.(Gly2045Arg)	Het
SNRNP200	NM_014014.4	Exon 13	–	–	c.1634G>A	p.(Arg545His)	Hom

RsID, reference SNP cluster ID; Zyg, zygocity.

Discussion

Retinitis pigmentosa due to mutations in the *SNRNP200* gene was first suggested to cause autosomal dominant disease[26,27] with a prevalence of 1.6% or more.[28] Some reports point to autosomal recessive inheritance, but no detailed phenotype description or clinical assessment of the respective patients is available (Table 5).[9,11]

The phenotype in the autosomal dominantly inherited *SNRRP200* mutation is characterized by an early but variable disease onset as demonstrated in family A. Night blindness is reported as the initial symptom starting between 5 and 15 years[19,27,29]; however, as known in autosomal dominant RP, variability with late onset can occur, as seen in patient II:2. Slow but inexorable progression has been described in patients with different mutations in the *SNRNP200* gene. Pan et al.[19] suggested that patients harboring the mutation c.3260C>T may be associated with a more severe phenotype than patients with the mutation c.2042G>A. We therefore compared the reported symptoms and age at onset, as well the phenotype, of all mutations published to date[4–12,19,27–36] in Table 5. Reduced vision and night blindness, less often visual field changes, are the most commonly reported symptoms. Age at onset varied between early childhood to early adolescence. The age at onset in our patient (II:2), in the sixth decade of life, is the oldest recorded to date. The published retinal phenotype descriptions are very limited, usually mentioning only "typical RP." Maculopathy was described in a few cases,[4,5,29,32] most of them carrying the same mutation as in family A; however, detailed or longitudinal imaging is not available in the published cases. Retinal function is described as rod-cone dysfunction except in one case with cone-rod dysfunction.[8] More affected families and detailed longitudinal data would be required in order to compare and correlate the phenotypic effect of certain mutations in the *SNRNP200* gene. Visual acuity ranges from subnormal to no light perception. Intrafamilial phenotype variability has been documented across three generations of a Chinese family.[37] As intrafamilial variability is reported in autosomal dominant RP, disease-modifying effects of identified SNPs in this report could be possible.[38–40]

Here we described the detailed phenotype in autosomal dominant RP in a Swiss family with the c.3260C>T missense mutation in the *SNRNP200* gene. Based on the reported patients in the literature published to date, this mutation may be a mutational "hot spot" as suggested by Benaglio et al.[6]

The index patient in our family A shows additional variants in *MYO7A* and *UNC119*, which do not segregate with the disease in the family and which do not result in auditory dysfunction. This patient does not show a more severe phenotype compared with the other affected family members (excepting his mother, who exhibited a less severe phenotype). Visual acuity is subnormal to reduced in the fourth decade to severely reduced in the seventh to eighth decade, with associated advanced visual field defects. Similarly to the intrafamilial variability reported by Liu et al.,[37] the mother of the index patient in family A exhibited a less severe functional loss at age 67 compared to affected family members of her generation. Disease progression was associated with cystoid macular edema (as previously documented in 10%–50% of patients with RP) within the inner nuclear layer only, due to a greater extent of macular atrophy affecting the outer nuclear

Table 4. Segregation Family A and B

	Family A				
Gene	Index A, III:1	II:1	III:2	II:4	II:5
	Affected	Affected	Unaffected	Affected	Affected
SNRNP200, c.3260C>T, p.(Ser1087Leu)	Het	Het	Reference	Het	Het
UNC119, c.502C>T, p.(Arg168Cys)	Het	Het	Het	Reference	NS
MYO7A, c.4739A>G, p.(Tyr1580Cys)	Het	Het	Het	Reference	NS
MYO7A, c.5380G>A, p.(Glu1794Lys)	Het	Reference	Reference	Reference	NS
	Family B				
	Index B	**Sister**	**Mother**	**Father**	
	Affected	Unaffected	Unaffected	Unaffected	
SNRNP200, c.1634G>A, p.(Arg545His)	Homo	Het	Het	Het	

Het, heterozygous; Homo, homozygous; NS, not sequenced.

Table 5. Phenotype Summary of Published Mutations in the *SNRNP200* Gene

Predicted Effect	Exon	Reference	Inheritance	Phenotype	Age at Onset	Presenting Symptoms	Retinal Phenotype	Maculopathy	ERG
p.I538M	13	Huang et al.[30] (2015)	Sporadic	RP	20	NA	NA	NA	NA
p.A542V	13	Bowne et al.[28] (2013)	AD	RP	5–21	NA	Typical RP.		
p.M544T	13	Huang et al.[30] (2015)	Sporadic	RP	20	NA	NA	NA	NA
pR545H	13	This study	AR*	RP	9	Vision reduction, night blindness.	Typical RP.		
p.V661L	15	Van Cauwenbergh et al.[31] (2017)	AD	RP	NA	NA	NA	NA	NA
c.2036+1G>T	15, splice donor site	Huang et al.[8] (2016)	AD	CORD	Early childhood	Poor vision.	Normal fundus.	NA	Moderately reduced rod responses, NR cone responses.
		Xu et al.[32] (2014)	Sporadic	RP	26	Poor vision, night blindness.	Attenuated vessels, pigment deposits.	Macular degeneration.	Severely reduced age 31.
p.R681C	16	Benaglio et al.[6] (2011)	AD	RP	NA	NA	NA	NA	NA
		Bowne et al.[28] (2013)	AD	RP	12–35	NA	Typical RP.+	NA	Normal to NR at age 24, 40.
		Xu et al.[32] (2014)	AD/sporadic	RP	Early childhood	Poor vision.	Typical RP.	None	Rod NR, cone moderately reduced (at age 5).
		Coussa et al.[7] (2015)	AD	RP	NA	NA	NA	NA	NA
		Van Cauwenbergh et al.[31] (2017)	AD	RP	NA	NA	NA	NA	NA
p.R681H	16	Bowne et al.[28] (2013)	AD	RP	13	NA	Typical RP	NA	NR at age 76.
		Pan et al.[19] (2014)	AD	RP	6 y	Night blindness.	Typical RP, rapid progression, high myopia (OCT: retinal thinning).	NA	Reduced
		Van Cauwenbergh et al.[31] (2017)	AD	RP	NA	NA	NA	NA	NA
		Benaglio et al.[6] (2011)	AD	RP	NA	NA	NA	NA	NA
p.R681L	16	de Castro-Miró et al.[33] (2014)	AD	RP	NA	NA	NA	NA	NA
p.P682S	16	Bowne et al.[28] (2013)	AD	RP	Not known	NA	NA	NA	NR at age 50.
p.V683L	16	Benaglio et al.[6] (2011)	AD	RP	NA	NA	NA	NA	NA
p.Y689C	16	Benaglio et al.[6] (2011)	AD	RP	NA	NA	NA	NA	NA
p.V708I	16	Coussa et al.[7] (2015)	AD	RP	NA	NA	NA	NA	NA
p.A787T	18	Xu et al.[32] (2014)	Sporadic	RP	Early childhood	Poor vision.	Typical RP.	None	NA
		Wang et al.[34] (2014)	AD	RP	19 (or age at test)	NA	NA	NA	NA
p.G865S	20	Patel et al.[35] (2016)	Sporadic	RD	NA	NA	NA	NA	NA
p.Q885E	20	Liu et al.[37] (2012)	AD	RP	10–15 y	Night blindness, visual field loss.	Typical RP, 2/8 angle closure glaucoma.	NA	Reduced to NR scotopic rod ERG.
c.2941-2A>G	22, splice acceptor site	Wang et al.[36] (2018)	AD	RP	NA	NA	NA	NA	NA

Table 5. Continued

Predicted Effect	Exon	Reference	Inheritance	Phenotype	Age at Onset	Presenting Symptoms	Retinal Phenotype	Maculopathy	ERG
p.P1045T	23	Wang et al.[9] (2013)	AR*	LCA	NA	NA	NA	NA	NA
		Bujakowski et al.[10] (2017)	AR†	RP	NA	NA	Typical RP (OCT: thinning).	Cystoid	NA
p.V1084F	24	Zhou et al.[12] (2018)	AD	eoHM	NA	NA	NA	NA	NA
p.S1087L	25	Zhao et al.[4,5] (2006, 2009)	AD	RP	14–20 y	Night blindness.	Variable expression.	In 2/11 patients examined at ages 49 and 51 y.	Rod cone dysfunction.
		Benaglio et al.[6] (2011)	AD	RP	NA	NA	NA	NA	NA
		Bowne et al.[28] (2013)	AD	RP	4–10	NA	Typical RP.		
		Pan et al.[19] (2014)	AD	RP	5–10 y	Night blindness.	Typical RP, rapid progression.	NA	Severely reduced age 34.
		Coussa et al.[7] (2015)	AD	RP	NA	NA	NA	NA	NA
		Ezquerra-Inchausti et al.[29] (2017)	AD	RP	NA	Night blindness, visual field loss, visual acuity loss.	Typical RP.	Macula edema in 4/10 reported.	NR
		This study	AD	RP	Early childhood to 55 y	Night blindness.	Typical RP.	Mild to severe atrophy with cystoid lesions on OCT.	Scotopic NR, photopic severely reduced to NR.
p. R 1090Q	25	Astuti et al.[11] (2018)	AR*	RD (? LCA or EORD)	Early infancy	Night blindness, visual field loss.	NA	NA	NA
p.R1090L	25	Li et al.[27] (2010)	AD	RP	7–8 y		Typical RP.		Rod cone dysfunction.
p.R1693C	36	Zhou et al.[12] (2018)	AD	eoHM	NA	NA	NA	NA	NA
p.N2103S	45	Patel et al.[35] (2016)	Sporadic	RD	NA	NA	NA	NA	NA

Mutations and variants of unknown significance from Supplementary Table S3 (Wang et al.[34]) not included. AD, autosomal dominant; AR, autosomal recessive; EORD, early-onset retinal dystrophy; ERG, electroretinogram.

* Homozygous.

† Both SNRNP200 and CNNM4 deletion.

layer (as observed in the older patients in this family). Bowne et al.[28] described preserved cone mosaics within the cystoid spaces (using adaptive optics scanning laser ophthalmoscopy) in patients with a *SNRNP200* mutation. Quantitative analysis of these cone mosaics revealed an increased cone spacing that nevertheless enabled a relatively good visual acuity of 20/63 in the examined eye,[28] a factor that may potentially explain the well-preserved visual acuity in our patient II:2 at age 67 years.

RP caused by *SNRNP200* mutations has not, to date, been associated with extraocular manifestations. Liu et al.[37] described a family with associated angle closure glaucoma in two of the five living patients with the c.3260C>T missense mutation. No other reported associations are known to date. Based on the patients described in our study together with other reports (Pan et al.[19]), we cannot confirm additional ocular or systemic manifestations. Therefore, angle closure glaucoma in these patients may not be attributable to the *SNRNP200* gene mutation.

We observed phenotypical differences in the affected patient with the homozygous mutation compared with the heterozygous mutation. Excluding the mildly affected patient II:2 in family A, disease onset and night blindness as the initial early symptom does not differ between the two families with the different inheritance pattern. However, the patient with the homozygous recessive mutation experienced an earlier reduction in visual acuity compared with the patients in family A carrying the heterozygous dominant mutation. Fundus changes are distinct, with speckled hypopigmentation, which has not been previously reported for *SNRNP200* mutations and was not visible in the dominant family (Fig. 4). Retinal function and morphology may also point to a more severe phenotype in the patient with the recessive mutation, although longitudinal data and additional affected patients are not available at the present time. In the present study, ff-ERG responses in this patient were already severely reduced by the age of 9 years. OCT showed increased retinal thinning relative to the much older patients with the dominant mutation in *SNRNP200* (Fig. 4; Table 2), although the presence of cystoid macular edema in the majority of the latter group of patients precludes a quantitative comparison.

Phenotype variability may be associated with both the dominant and recessive modes of inheritance of mutations in the *SNRNP200* gene. Wang et al.[9] described the case of one patient with LCA caused by a homozygous mutation (c.3133C>A, p.(Pro1045Thr)) in the *SNRNP200* gene (no clinical details available).[9] Astuti et al.[11] described a likely pathogenic, homozygous mutation c.3269C>A (p.(Arg1090Gln)) in a consanguineous family from Pakistan with an affected child and his aunt, with the former showing an early disease onset with a visual acuity reduction to 1.0 logMAR at the age of 15. The phenotype of the aunt was not described. No other details or functional data are available from these families of autosomal recessive inheritance.

The patient reported by Bujakowska et al.[10] carried a compound heterozygous deletion in the *SNRNP200* and *CNNM4* genes. The authors did not discuss which of the gene changes is causative. Two patients reported there were carrying a heterozygous deletion of approximately 1.1 Mb including 20 genes. Two of them, *SNRNP200* and *CNNM4*, are known retinal disease genes. Both of the two patients carry an additional point mutation in either *CNNM4* or *SNRNP200*, compatible with an autosomal recessive mode of inheritance in both cases.

Both autosomal dominant and recessive inheritance patterns are already known for other genes associated with nonsyndromic retinal dystrophies: *Best1*, *IMPDH1*, *NR2E3*, *NRL*, *SAG*, *RDH12*, *RP1*, *RPE65* (summarized in Verbakel et al.[41]). Similarly to the above genes, autosomal dominant *SNRNP200* mutations appear to be associated with a less severe RP disease course compared to the autosomal recessive inheritance.

The p.(Arg545His) substitution in our patient in family B lies in the more important and active N-terminal cassette of the U5 small nuclear ribonucleoprotein 200-kDa helicase (BRR2), which consists of two prototypical RecA-like ATPase domains.[42] The C-terminal cassette of BRR2 serves as an intramolecular cofactor. The mutation lies in the first RecA domain which forms the first contact with ATP, the energy source of the helicase. Due to this position, the effect of p.(Arg545His) may be similar to p.(Ser1087Leu), which showed decreased RNA binding and reduced helicase activity[4] and is in close proximity to other autosomal recessive inherited variants (Fig. 1). In addition, in close proximity to amino acid position 545 of BRR2, other variants causing a retinal phenotype have been published: p.(Ile538-Met) (simplex RP),[30] p.(Ala542Val) (autosomal dominant RP),[28] and p.(Met544Thr) (simplex RP).[30] A similar situation is found at amino acid position 1090 in the Sec63 domain of the protein. There, a dominant as well as a recessive missense exchange was described by Li et al.[27] and Astuti et al.,[11] respectively. We believe that a dominant variant leads to a dominant negative effect in the protein, while a recessive variant leads to loss of protein function. This is supported by the findings of Bujakowska et al.,[10] who described a heterozygous deletion of *SNRNP200* in an unaffected family member. Thus, haploinsufficiency seems unlikely for dominant variants in *SNRNP200*. Taken together, mutations in this protein domain seem to cause the retinal phenotype and are responsible for autosomal recessive RP, as in the index patient of family B. Only two missense mutations out of 34 *SNRNP200* variants from 47 publications, which are listed in HGMD, have been functionally characterized p.S1087L and p.R1090L.[3] The respective functional studies for the two variants were performed in HeLa cells using beta globin RNA as the target of splicing. The results indicate some deleterious effect of the two amino acid substitutions but only when the endogenous *SNRNP200* expression is knocked down. Therefore, we believe that currently no proper functional assay is available in order to study the effect of amino acid substitutions in SNRNP200 with relevance to ocular or retinal tissue or cells.

In summary, this report describes a novel recessive mutation c.1634G>A (p.(Arg545His)) in the *SNRNP200* gene associated with a phenotype typical for juvenile RP. Functional analysis of this sequence variant will be required to provide evidence for the association with disease. Such functional studies are also necessary prior to the application of gene therapeutic approaches in patients. Visual dysfunction may be more severe than in patients with the dominantly inherited SNRNP200 mutation. However, detailed genotype–phenotype correlation and verification of the mechanisms leading to autosomal recessive or dominant disease will be possible only through future functional studies. Awareness of the possibility of dominant and recessive inheritance pattern and severe phenotypes such as LCA should be taken into account when counseling patients and family members.

Acknowledgments

Supported by a grant from the Swiss National Science Foundation (Grant No. 320030_138507) and from Velux Stiftung Switzerland (WB).

Disclosure: **C. Gerth-Kahlert**, None; **S. Koller**, None; **J.V.M. Hanson**, None; **L. Baehr**, None; **A. Tiwari**, None; **F. Kivrak-Pfiffner**, None; **A. Bahr**, None; **W. Berger**, None

References

1. Laggerbauer B, Achsel T, Luhrmann R. The human U5-200kD DEXH-box protein unwinds U4/U6 RNA duplices in vitro. *Proc Natl Acad Sci U S A*. 1998;95:4188–4192.
2. Raghunathan PL, Guthrie C. RNA unwinding in U4/U6 snRNPs requires ATP hydrolysis and the DEIH-box splicing factor Brr2. *Curr Biol*. 1998;8:847–855.
3. Cvackova Z, Mateju D, Stanek D. Retinitis pigmentosa mutations of SNRNP200 enhance cryptic splice-site recognition. *Hum Mutat*. 2014;35:308–317.
4. Zhao C, Bellur DL, Lu S, et al. Autosomal-dominant retinitis pigmentosa caused by a mutation in SNRNP200, a gene required for unwinding of U4/U6 snRNAs. *Am J Hum Genet*. 2009;85:617–627.
5. Zhao C, Lu S, Zhou X, Zhang X, Zhao K, Larsson C. A novel locus (RP33) for autosomal dominant retinitis pigmentosa mapping to chromosomal region 2cen-q12.1. *Hum Genet*. 2006;119:617–623.
6. Benaglio P, McGee TL, Capelli LP, Harper S, Berson EL, Rivolta C. Next generation sequencing of pooled samples reveals new SNRNP200 mutations associated with retinitis pigmentosa. *Hum Mutat*. 2011;32:E2246–E2258.
7. Coussa RG, Chakarova C, Ajlan R, et al. Genotype and phenotype studies in autosomal dominant retinitis pigmentosa (adRP) of the French Canadian founder population. *Invest Ophthalmol Vis Sci*. 2015;56:8297–8305.
8. Huang L, Xiao X, Li S, et al. Molecular genetics of cone-rod dystrophy in Chinese patients: new data from 61 probands and mutation overview of 163 probands. *Exp Eye Res*. 2016;146:252–258.
9. Wang X, Wang H, Sun V, et al. Comprehensive molecular diagnosis of 179 Leber congenital amaurosis and juvenile retinitis pigmentosa patients by targeted next generation sequencing. *J Med Genet*. 2013;50:674–688.
10. Bujakowska KM, Fernandez-Godino R, Place E, et al. Copy-number variation is an important contributor to the genetic causality of inherited retinal degenerations. *Genet Med*. 2017;19:643–651.
11. Astuti GDN, van den Born LI, Khan MI, et al. Identification of inherited retinal disease-associated genetic variants in 11 candidate genes. *Genes (Basel)*. 2018;9:E21.
12. Zhou L, Xiao X, Li S, Jia X, Zhang Q. Frequent mutations of RetNet genes in eoHM: further confirmation in 325 probands and comparison with late-onset high myopia based on exome sequencing. *Exp Eye Res*. 2018;171:76–91.
13. Hood DC, Bach M, Brigell M, et al. ISCEV standard for clinical multifocal electroretinography (mfERG) (2011 edition). *Doc Ophthalmol*. 2012;124:1–13.
14. Lek M, Karczewski KJ, Minikel EV, et al. Analysis of protein-coding genetic variation in 60,706 humans. *Nature*. 2016;536:285–291.
15. Klambauer G, Schwarzbauer K, Mayr A, et al. cn.MOPS: mixture of Poissons for discovering copy number variations in next-generation sequencing data with a low false discovery rate. *Nucleic Acids Res*. 2012;40:e69.
16. D'Aurizio R, Pippucci T, Tattini L, Giusti B, Pellegrini M, Magi A. Enhanced copy number variants detection from whole-exome sequencing data using EXCAVATOR2. *Nucleic Acids Res*. 2016;44:e154.
17. Haghighi A, Tiwari A, Piri N, et al. Homozygosity mapping and whole exome sequencing reveal a novel homozygous COL18A1 mutation causing Knobloch syndrome. *PLoS One*. 2014;9:e112747.
18. McCulloch DL, Marmor MF, Brigell MG, et al. ISCEV Standard for full-field clinical electroretinography (2015 update). *Doc Ophthalmol*. 2015;130:1–12.
19. Pan X, Chen X, Liu X, et al. Mutation analysis of pre-mRNA splicing genes in Chinese families with retinitis pigmentosa. *Mol Vis*. 2014;20:770–779.
20. Tavtigian SV, Deffenbaugh AM, Yin L, et al. Comprehensive statistical study of 452 BRCA1 missense substitutions with classification of eight recurrent substitutions as neutral. *J Med Genet*. 2006;43:295–305.
21. Sim NL, Kumar P, Hu J, Henikoff S, Schneider G, Ng PC. SIFT web server: predicting effects of amino acid substitutions on proteins. *Nucleic Acids Res*. 2012;40:W452–W457.
22. Schwarz JM, Cooper DN, Schuelke M, Seelow D. MutationTaster2: mutation prediction for the deep-sequencing age. *Nat Methods*. 2014;11:361–362.
23. Adzhubei IA, Schmidt S, Peshkin L, et al. A method and server for predicting damaging missense mutations. *Nat Methods*. 2010;7:248–249.
24. Stone EA, Sidow A. Physicochemical constraint violation by missense substitutions mediates impairment of protein function and disease severity. *Genome Res*. 2005;15:978–986.
25. Raponi M, Kralovicova J, Copson E, et al. Prediction of single-nucleotide substitutions that result in exon skipping: identification of a splicing silencer in BRCA1 exon 6. *Hum Mutat*. 2011;32:436–444.
26. Zhang L, Xu T, Maeder C, et al. Structural evidence for consecutive Hel308-like modules in the spliceosomal ATPase Brr2. *Nat Struct Mol Biol*. 2009;16:731–739.
27. Li N, Mei H, MacDonald IM, Jiao X, Hejtmancik JF. Mutations in ASCC3L1 on 2q11.2 are associated with autosomal dominant retinitis pigmentosa in a Chinese family. *Invest Ophthalmol Vis Sci*. 2010;51:1036–1043.
28. Bowne SJ, Sullivan LS, Avery CE, et al. Mutations in the small nuclear riboprotein 200 kDa gene (SNRNP200) cause 1.6% of autosomal dominant retinitis pigmentosa. *Mol Vis*. 2013;19:2407–2417.
29. Ezquerra-Inchausti M, Barandika O, Anasagasti A, Irigoyen C, Lopez de Munain A, Ruiz-Ederra J. High prevalence of mutations affecting the splicing process in a Spanish cohort with autosomal dominant retinitis pigmentosa. *Sci Rep*. 2017;7:39652.
30. Huang XF, Huang F, Wu KC, et al. Genotype-phenotype correlation and mutation spectrum in a large cohort of patients with inherited retinal dystrophy revealed by next-generation sequencing. *Genet Med*. 2015;17:271–278.
31. Van Cauwenbergh C, Coppieters F, Roels D, et al. Mutations in splicing factor genes are a major cause of autosomal dominant retinitis pigmentosa in Belgian families. *PLoS One*. 2017;12:e0170038.
32. Xu Y, Guan L, Shen T, et al. Mutations of 60 known causative genes in 157 families with retinitis pigmentosa based on exome sequencing. *Hum Genet*. 2014;133:1255–1271.
33. de Castro-Miro M, Pomares E, Lores-Motta L, et al. Combined genetic and high-throughput strategies for molecular diagnosis of inherited retinal dystrophies. *PLoS One*. 2014;9:e88410.
34. Wang J, Zhang VW, Feng Y, et al. Dependable and efficient clinical utility of target capture-based deep sequencing in molecular diagnosis of retinitis pigmentosa. *Invest Ophthalmol Vis Sci*. 2014;55:6213–6223.
35. Patel N, Aldahmesh MA, Alkuraya H, et al. Expanding the clinical, allelic, and locus heterogeneity of retinal dystrophies. *Genet Med*. 2016;18:554–562.
36. Wang L, Zhang J, Chen N, et al. Application of whole exome and targeted panel sequencing in the clinical molecular diagnosis of 319 Chinese families with inherited retinal dystrophy and comparison study. *Genes (Basel)*. 2018;9:360.
37. Liu T, Jin X, Zhang X, et al. A novel missense SNRNP200 mutation associated with autosomal dominant retinitis pigmentosa in a Chinese family. *PLoS One*. 2012;7:e45464.

Investigative Ophthalmology & Visual Science

38. Berson EL, Rosner B, Sandberg MA, Dryja TP. Ocular findings in patients with autosomal dominant retinitis pigmentosa and a rhodopsin gene defect (Pro-23-His). *Arch Ophthalmol*. 1991;109:92–101.
39. Venturini G, Rose AM, Shah AZ, Bhattacharya SS, Rivolta C. CNOT3 is a modifier of PRPF31 mutations in retinitis pigmentosa with incomplete penetrance. *PLoS Genet*. 2012; 8:e1003040.
40. Maubaret CG, Vaclavik V, Mukhopadhyay R, et al. Autosomal dominant retinitis pigmentosa with intrafamilial variability and incomplete penetrance in two families carrying mutations in PRPF8. *Invest Ophthalmol Vis Sci*. 2011;52:9304–9309.
41. Verbakel SK, van Huet RAC, Boon CJF, et al. Non-syndromic retinitis pigmentosa. *Prog Retin Eye Res*. 2018;66:157–186.
42. Strong S, Liew G, Michaelides M. Retinitis pigmentosa-associated cystoid macular oedema: pathogenesis and avenues of intervention. *Br J Ophthalmol*. 2017;101:31–37.
43. Zhang X, Lai TYY, Chiang SWY, et al. Contribution of *SNRNP200* sequence variations to retinitis pigmentosa. *Eye*. 2013;27:1204–1213.

Investigative Ophthalmology & Visual Science